Quality Improvement Study

Medicine®

OPEN

Identification of the differential expression of genes and upstream microRNAs in small cell lung cancer compared with normal lung based on bioinformatics analysis

Xiuwei Li, MD[a], Chao Ma, MD[b], Huan Luo, MD[c], Jian Zhang, MD[a], Jinan Wang, MD[a], Hongtao Guo, MD[a,*]

Abstract

Small cell lung cancer (SCLC) is one of the most lethal cancer, mainly attributing to its high tendency to metastasis. Mounting evidence has demonstrated that genes and microRNAs (miRNAs) are related to human cancer onset and progression including invasion and metastasis.

An eligible gene dataset and an eligible miRNA dataset were downloaded from the Gene Expression Omnibus (GEO) database based our screening criteria. Differentially expressed genes (DE-genes) or DE-miRNAs for each dataset obtained by the R software package. The potential target genes of the top 10 DE-miRNAs were predicted by multiple databases. For annotation, visualization and integrated discovery, Metascape 3.0 was introduced to perform enrichment analysis for the DE-genes and the predicted target genes of the selected top 10 DE-miRNAs, including Pathway and Process Enrichment Analysis or protein–protein interaction enrichment analysis. The intersection of predicted target genes and DE-genes was taken as the final DE-genes. Then apply the predicted miRNAs-targets relationship of top 10 DE-miRNAs to the final DE-genes to gain more convinced DE-miRNAs, DE-genes and their one to one relationship.

GSE19945 (miRNA microarray) and GSE40275 (gene microarray) datasets were selected and downloaded. 56 DE-miRNAs and 861 DE-genes were discovered. 297 miRNAs-targets relationships (284 unique genes) were predicted as the target of top 10 upregulating DE-miRNAs. 245 miRNAs-targets relationships (238 unique genes) were identified as the target of top 10 downregulating DE-miRNAs. The key results of enrichment analysis include protein kinase B signaling, transmembrane receptor protein tyrosine kinase signaling pathway, negative regulation of cell differentiation, response to growth factor, cellular response to lipid, muscle structure development, response to growth factor, signaling by Receptor Tyrosine Kinases, epithelial cell migration, cellular response to organic cyclic compound, Cell Cycle (Mitotic), DNA conformation change, cell division, DNA replication, cell cycle phase transition, blood vessel development, inflammatory response, *Staphylococcus aureus* infection, leukocyte migration, and myeloid leukocyte activation. Differential expression of genes-upstream miRNAs (RBMS3-hsa-miR-7–5p, NEDD9-hsa-miR-18a-5p, CRIM1-hsa-miR-18a-5p, TGFBR2-hsa-miR-9–5p, MYO1C-hsa-miR-9–5p, KLF4-hsa-miR-7–5p, EMP2-hsa-miR-1290, TMEM2-hsa-miR-18a-5p, CTGF-hsa-miR-18a-5p, TNFAIP3-hsa-miR-18a-5p, THBS1-hsa-miR-182–5p, KPNA2-hsa-miR-144–3p, GPR137C-hsa-miR-1–3p, GRIK3-hsa-miR-144–3p, and MTHFD2-hsa-miR-30a-3p) were identified in SCLC.

RBMS3, NEDD9, CRIM1, KPNA2, GPR137C, GRIK3, hsa-miR-7–5p, hsa-miR-18a-5p, hsa-miR-144–3p, hsa-miR-1–3p along with the pathways included protein kinase B signaling, muscle structure development, Cell Cycle (Mitotic) and blood vessel development may gain a high chance to play a key role in the prognosis of SCLC, but more studies should be conducted to reveal it more clearly.

Abbreviations: CRIM1 = Cysteine Rich Transmembrane BMP Regulator 1, CTGF = Cellular Communication Network Factor 2, DE = differentially expressed, EMP2 = epithelial membrane protein 2, GEO = Gene Expression Omnibus, GO = gene ontology, GPR137C = G protein-coupled receptor 137C, GRIK3 = glutamate ionotropic receptor kainate type subunit 3, KEGG = Kyoto encyclopedia of genes and genomes, KLF4 = Kruppel like factor 4, KPNA2 = Karyopherin subunit alpha 2, miR = microRNA, miRNA = microRNA, MTHFD2 = methylenetetrahydrofolate dehydrogenase (NADP+ dependent) 2, methenyltetrahydrofolate cyclohydrolase, MYO1C = myosin IC, NCBI = National Center for Biotechnology Information, NEDD9 = neural precursor cell expressed,

Editor: Eric Bush.

Data availability: All data reported have been obtained from GEO database.

This study was funded by Zhengzhou University Overseas Virtual Research Institute Special Fund, Zhengzhou University.

The authors have no conflicts of interest to disclose.

[a] Department of Radiotherapy, Zhoukou Central Hospital, Zhoukou, China, [b] Department of Cardiology, [c] Department of Ophthalmology, Campus Virchow, Charité–Universitätsmedizin Berlin, Berlin, Germany.

[*] Correspondence: Hongtao Guo, Department of Radiotherapy, Zhoukou Central Hospital, Zhoukou, China (e-mail: zkszxyyflk@outlook.com).

How to cite this article: Li X, Ma C, Luo H, Zhang J, Wang J, Guo H. Identification of the differential expression of genes and upstream microRNAs in small cell lung cancer compared with normal lung based on bioinformatics analysis. Medicine 2020;99:11(e19086).

Received: 17 May 2019 / Received in final form: 8 January 2020 / Accepted: 9 January 2020

http://dx.doi.org/10.1097/MD.0000000000019086

developmentally down-regulated 9, NSCLC = non-small-cell lung carcinoma, RBMS3 = RNA binding motif single stranded interacting protein 3, SCLC = small cell lung cancer, TGFBR2 = transforming growth factor beta receptor 2, THBS1 = thrombospondin 1, TMEM2 = cell migration inducing hyaluronidase 2, TNFAIP3 = TNF alpha induced protein 3.

Keywords: bioinformatics analysis, differential expression, gene, lung cancer, microRNA, small cell lung cancer

1. Introduction

Small cell lung cancer (SCLC) is a high grade poorly differentiated neuroendocrine carcinoma of the lung, which represents approximately 15% of bronchogenic carcinomas and up to 25% of lung cancer deaths.[1,2] SCLC is associated with early metastasis and poor patient survival.[3] Regardless of stage, the current prognosis for patients with SCLC is unsatisfactory despite improvements in diagnosis and therapy made during the past 25 years. Without treatment, SCLC has the most aggressive clinical course of any type of pulmonary tumor, with median survival from diagnosis of only 2 to 4 months.[2] Overall survival in SCLC is dismal with a 5-year survival of ~2% for extensive stage metastatic disease, which comprises 70% of cases at initial diagnosis.[4] SCLC is more responsive to chemotherapy and radiation therapy than other cell types of lung cancer; however, a cure is difficult to achieve because SCLC has a greater tendency to be widely disseminated by the time of diagnosis.[2]

In view of the potentially limited impact of the further developments of standard therapeutic regimens on patient survival, the development of targeted therapies based on a better understanding of the molecular basis of the disease is urgently needed.[5] At the genetic level, SCLC appears to be very heterogeneous, although somatic mutations targeting classical oncogenes and tumor suppressors, such as MYC, TP53, and RB1 have been reported, more genes involved in SCLC are waiting for us to explore furtherer.[5] MicroRNAs (miRNAs) are a group of small endogenous single-stranded non-coding RNAs, ~21 to 25 nucleotides in length.[6] MiRNAs can negatively modulate gene expression via binding to the 3′-untranslated region of messenger RNA (mRNA), thereby leading to direct degradation of mRNA or suppression of protein translation. Through this approach, miRNAs are involved in regulation of many biological processes such as proliferation, apoptosis, cell cycle and differentiation, and DNA repair.[7] Over the past decades, mounting studies have demonstrated that miRNA is frequently abnormally expressed in various types of cancer including SCLC, and the dysregulation of miRNA plays a paramount role in tumorigenesis, invasion and metastasis.[8,9] However, research exploring Differential expression miRNAs in SCLC based on large-scale human tissues are rarely seen.

With the rapid development of gene chip and RNA sequencing technologies, Gene Expression Omnibus (GEO) gradually plays an important role in the bioinformatic analysis.[10] It can provide us with novel clues for discovering reliable genes and miRNAs. In the present study, we explore the differential expression of genes and miRNAs in SCLC and normal lung tissue and the potential molecular mechanisms related to them based on GEO database and comprehensive bioinformatic analysis.

2. Materials and methods

2.1. MiRNA and gene microarrays

In the discovery step, we log in to the National Center for Biotechnology Information (NCBI) GEO database (https://www.ncbi.nlm.nih.gov/geo) to look for the microarrays we need. We only considered datasets that compared the miRNA and gene expression in SCLC tissue with normal lung tissue. Besides, the containing of samples in such datasets should be over forty. The titles and abstracts of these datasets were screened, and the full information of the datasets of interest was further evaluated. We will choose one most suitable miRNA and gene microarrays respectively.

2.2. Screening for DE-miRNAs and DE-genes

Data were normalized using the normalizeBetweenArray function from R package "LIMMA" from the bioconductor project. The miRNA and gene differential expression analysis were conducted using the limma software package in the Bioconductor package (http://www.bioconductor.org/). The related codes were put into R, and the DE-miRNAs and DE-genes in SCLC tumor samples compared to normal lung samples were analyzed through the limma package. FDR (False Discovery Rate) adjusted P-value $< .001$ and $|\text{fold change (FC)}| > 2$ were set as the thresholds for identifying DE-miRNAs and DE-genes. The upregulated or downregulated DE-miRNAs and DE-genes were sorted according to the size of their |fold change (FC)|.

2.3. Prediction of target genes for DE-miRNAs

The potential target genes of the top 10 most upregulated and downregulated DE-miRNAs were obtained from the intersection of prediction of miRTarBase Release 7.0 (http://mirtarbase.mbc.nctu.edu.tw), TargetScan Release 7.2 (http://www.targetscan.org) and miRDB Version 5.0 (http://mirdb.org). miRTarBase Release 7.0 is an experimentally validated microRNA-target interactions database, which is updated on September 15, 2017. TargetScan Release 7.2 updated on March 2018, and it is a web server that predicts biological targets of microRNAs by searching for the presence of sites that match the seed region of each miRNA. miRDB Version 5.0 released on August 2014, it is an online database for miRNA target prediction and functional annotations.

2.4. Enrichment analysis

The monthly updated database for annotation, visualization and integrated discovery (Metascape 3.0, http://metascape.org) was introduced to perform enrichment analysis for the DE-genes and the predicted target genes of the selected 20 DE-miRNAs, including Pathway and Process Enrichment Analysis or Protein-protein Interaction Enrichment Analysis. All genes in the genome have been used as the enrichment background. Terms with a P-value $< .01$, a minimum count of 3, and an enrichment factor $>$ 1.5 (the enrichment factor is the ratio between the observed counts and the counts expected by chance) are collected and grouped into clusters based on their membership similarities. More specifically, P-values are calculated based on the accumulative hypergeometric distribution,[11] and q-values are calculated using the Banjamini–Hochberg procedure to account

for multiple testings.[12] Kappa scores[13] are used as the similarity metric when performing hierarchical clustering on the enriched terms, and sub-trees with a similarity of >0.3 are considered a cluster. The most statistically significant term within a cluster is chosen to represent the cluster. For each given gene list, protein–protein interaction enrichment analysis has been carried out with the following databases: BioGrid6, InWeb_IM7, OmniPath8. The resultant network contains the subset of proteins that form physical interactions with at least one other member in the list. If the network contains between 3 and 500 proteins, the Molecular Complex Detection (MCODE) algorithm9 has been applied to identify densely connected network components. Pathway and process enrichment analysis has been applied to each MCODE component independently.

2.5. Conjoint analysis of DE-miRNAs and DE-genes

In this step, due to the special regulation mechanism of miRNAs, we intersect the upregulated DE-genes and the predicted target genes of top 10 most downregulated DE-miRNAs, apply the prediction miRNAs-targets relationship of top 10 most downregulated DE-miRNAs to the intersection. Then, intersect the downregulated DE-genes and the predicted target genes of top 10 most upregulated DE-miRNAs, apply the prediction miRNAs-targets relationship of top 10 most upregulated DE-miRNAs to the intersection. In order to gain more convincing DE-miRNAs, DE-genes, and their one to one relationship.

2.6. Statistical analysis

The results were shown as mean ± SD. Differences between two groups were estimated using unpaired Student's t test. A two-tailed value of $P < .05$ or FDR adjusted P-value $< .05$ was considered as statistically significant.

3. Results

3.1. Microarrays

We found eight datasets regarding normal lung tissue compared with SCLC tissue. But six of them have more smaller simply size, so finally, only GSE19945 and GSE40275 datasets were selected to further study. The dataset GSE19945 was based on the platform of GPL9948 (Agilent Human 0.6K miRNA Microarray G4471A), contained 8 human normal lung samples and 35 human SCLC samples. GSE40275 is a GPL15974 platform (Human Exon 1.0 ST Array)-based dataset, contained 43 human normal lung samples and 15 human SCLC samples (Table 1).

3.2. Identification of DE-miRNAs and DE-genes

To identify DE-miRNAs and DE-genes from GSE19945 and GSE40275, respectively, we conducted normalized and differential expression analysis using limma software package, data before and after normalization were shown in Figure 1. Based on this analysis and our screening criteria, a total of 56 miRNAs were found to be significantly differentially expressed in human SCLC samples when compared to human normal lung samples, including 24 upregulated and 32 downregulated miRNAs. Furthermore, amount to 861 significantly differentially expressed genes were discovered, of which 350 upregulated and 511 downregulated. For better visualization, heatmap of DE-genes were provided in Figure 2, volcano plots of these DE-miRNAs and DE-genes were provided in Figure 3, the top 20 most upregulated and top 20 most downregulated miRNAs and genes were ranked by |fold change (FC)| in Tables 2–5.

3.3. The target genes of DE-miRNAs

The top 10 upregulated DE-miRNAs were hsa-miR-9–3p, hsa-miR-1290, hsa-miR-7–5p, hsa-miR-183–5p, hsa-miR-130b-3p, hsa-miR-9–5p, hsa-miR-301b-3p, hsa-miR-96–5p, hsa-miR-182–5p, and hsa-miR-18a-5p. The top 10 downregulated DE-miRNAs were hsa-miR-144–5p, hsa-miR-1–3p, hsa-miR-30a-3p, hsa-miR-144–3p, hsa-miR-486–5p, hsa-miR-451a, hsa-miR-126–5p, hsa-miR-145–5p, hsa-miR-145–3p, hsa-miR-126–3p. We searched for the above miRNAs target genes in databases miRTarBase, TargetScan and miRDB respectively. The genes predicted by the three databases at the same time were identified as target genes for DE-miRNAs. Finally, 297 miRNAs-targets relationships (284 unique genes) were simultaneously predicted by three databases as the target of top 10 upregulating DE-miRNAs. In the same way, 245 miRNAs-targets relationships (238 unique genes) were identified as the target of top 10 downregulating DE-miRNAs. For better visualization, miRNAs-genes network of these DE-miRNAs were provided in Figure 4,

4. Enrichment analysis

4.1. Pathway and process enrichment analysis

For the predicted target genes of DE-miRNAs and the DE-genes, pathway and process enrichment analysis have been carried out with the following ontology sources: Kyoto Encyclopedia of Genes and Genomes (KEGG) Pathway, Gene Ontology (GO) Biological Processes, Reactome Gene Sets, Canonical Pathways, and CORUM. The top 5 Pathway and Process Enrichment Analysis for target genes of the 10 upregulated DE-miRNAs included protein kinase B signaling, transmembrane receptor protein tyrosine kinase signaling pathway, negative regulation of cell differentiation, response to growth factor, cellular response to lipid. All of the above belong to the GO Biological Processes category. The top 5 Pathway and Process Enrichment Analysis for target genes of the top 10 downregulated DE-miRNAs included muscle structure development, response to growth factor, Signaling by Receptor Tyrosine Kinases, epithelial cell migration, cellular response to organic cyclic compound. Except

Table 1

Basic information of the selected datasets.

Datasets (type)	Platform	The number of human normal lung samples	The number of human small cell lung cancer samples	Download web link
GSE19945 (miRNA microarray)	GPL9948	8	35	https://www.ncbi.nlm.nih.gov/geo/query/acc.cgi?acc=GSE19945
GSE40275 (gene microarray)	GPL15974	43	15	https://www.ncbi.nlm.nih.gov/geo/query/acc.cgi?acc=GSE40275

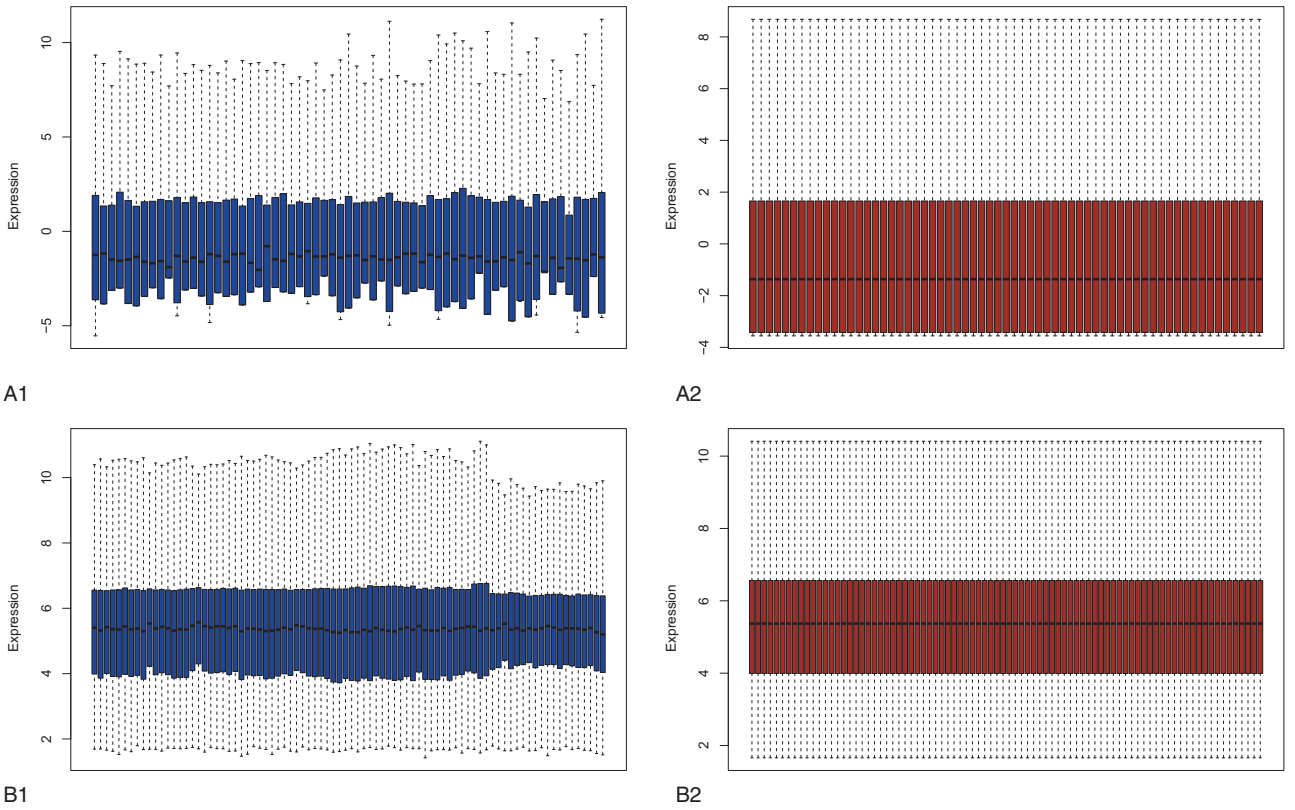

Figure 1. Normalization of datasets GSE19945 (A) and GSE40275 (B). (A1 and B1) Data before normalization; (A2 and B2) data after normalization.

for Signaling by Receptor Tyrosine Kinases (Reactome Gene Sets category), all above belong to the GO Biological Processes category. The top 5 Pathway and Process Enrichment Analysis for the upregulated DE-genes included Cell Cycle (Mitotic), DNA conformation change, cell division, DNA replication and cell cycle phase transition. They all belong to the GO Biological Processes category, except that Cell Cycle (Mitotic) belongs to Reactome Gene Sets category. The top 5 Pathway and Process Enrichment Analysis for the downregulated DE-genes included blood vessel development, inflammatory response, *Staphylococcus aureus* infection, leukocyte migration and myeloid leukocyte activation. Only *S aureus* infection belongs to the KEGG Pathway category, others belong to GO Biological Processes. For more details on Pathway and Process Enrichment Analysis, see Tables 6–9. To further capture the relationships between the terms, a subset of enriched terms have been selected and rendered as a network plot, where terms with a similarity >0.3 are connected by edges. We select the terms with the best *P*-values from each of the 20 clusters, with the constraint that there are no more than 15 terms per cluster and no more than 250 terms in total. The networks of enriched terms are visualized using Cytoscape (Figs. 5 and 6), where each node represents an enriched term and is colored first by its cluster ID (Fig. 5A1 and B1, Fig. 6A1 and B1) and then by its *P*-value (Fig. 5A2 and B2, Fig. 6A2 and B2).

4.2. Protein–protein interaction enrichment analysis

For the upregulated and downregulated DE-genes, protein–protein interaction enrichment analysis has been carried out with the following databases: BioGrid, InWeb_IM, OmniPath. The resultant network contains the subset of proteins that form physical interactions with at least one other member in the list. If the network contains between 3 and 500 proteins, the Molecular Complex Detection (MCODE) algorithm has been applied to identify densely connected network components. The MCODE networks identified for the DE-genes have been gathered and are shown in Figure 7.

Pathway and process enrichment analysis has been applied to each MCODE component independently, and the three best-scoring terms by *P*-value have been retained as the functional description of the corresponding components, shown in Tables 10 and 11 underneath corresponding network plots within Figure 7.

4.3. Conjoint analysis of DE-miRNAs and DE-genes

We got four upregulated and eleven downregulated DE-genes and their upstream miRNAs in this step. The downregulated DE-genes and their upstream miRNAs are as below, RBMS3 (RNA Binding Motif Single Stranded Interacting Protein 3)-hsa-miR-7–5p, NEDD9 (Neural Precursor Cell Expressed, Developmentally Down-Regulated 9)-hsa-miR-18a-5p, CRIM1 (Cysteine Rich Transmembrane BMP Regulator 1)-hsa-miR-18a-5p, TGFBR2 (Transforming Growth Factor Beta Receptor 2)-hsa-miR-9–5p, MYO1C (Myosin IC)-hsa-miR-9–5p, KLF4 (Kruppel Like Factor 4)-hsa-miR-7–5p, EMP2 (Epithelial Membrane Protein 2)-hsa-miR-1290, TMEM2 (Cell Migration Inducing Hyaluronidase 2)-hsa-miR-18a-5p, CTGF (Cellular Communication Network Factor 2)-hsa-miR-18a-5p, TNFAIP3 (TNF Alpha Induced Protein 3)-hsa-miR-18a-5p,

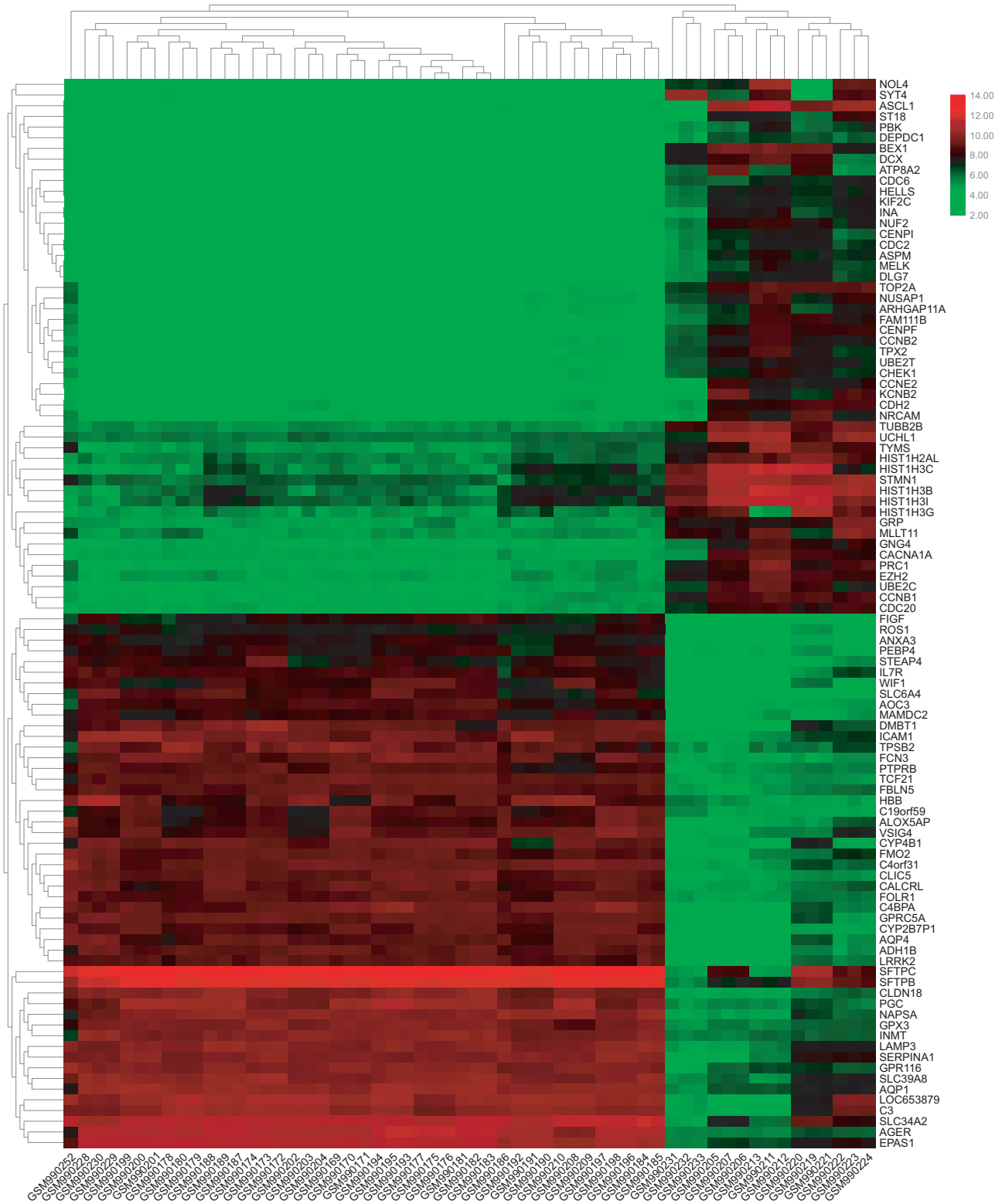

Figure 2. The heatmap of differentially expressed genes.

THBS1 (Thrombospondin 1)-hsa-miR-182–5p. We found the upregulated DE-genes and their upstream miRNAs, KPNA2 (Karyopherin Subunit Alpha 2)-hsa-miR-144–3p, GPR137C (G Protein-Coupled Receptor 137C)- hsa-miR-1–3p, GRIK3 (Glutamate Ionotropic Receptor Kainate Type Subunit 3)-hsa-miR-144–3p and MTHFD2 (Methylenetetrahydrofolate Dehydrogenase (NADP+ Dependent) 2, Methenyltetrahydrofolate Cyclohydrolase)-hsa-miR-30a-3p. The conjoint analysis was more convinced (Fig. 8). Details are shown in Tables 12 and 13.

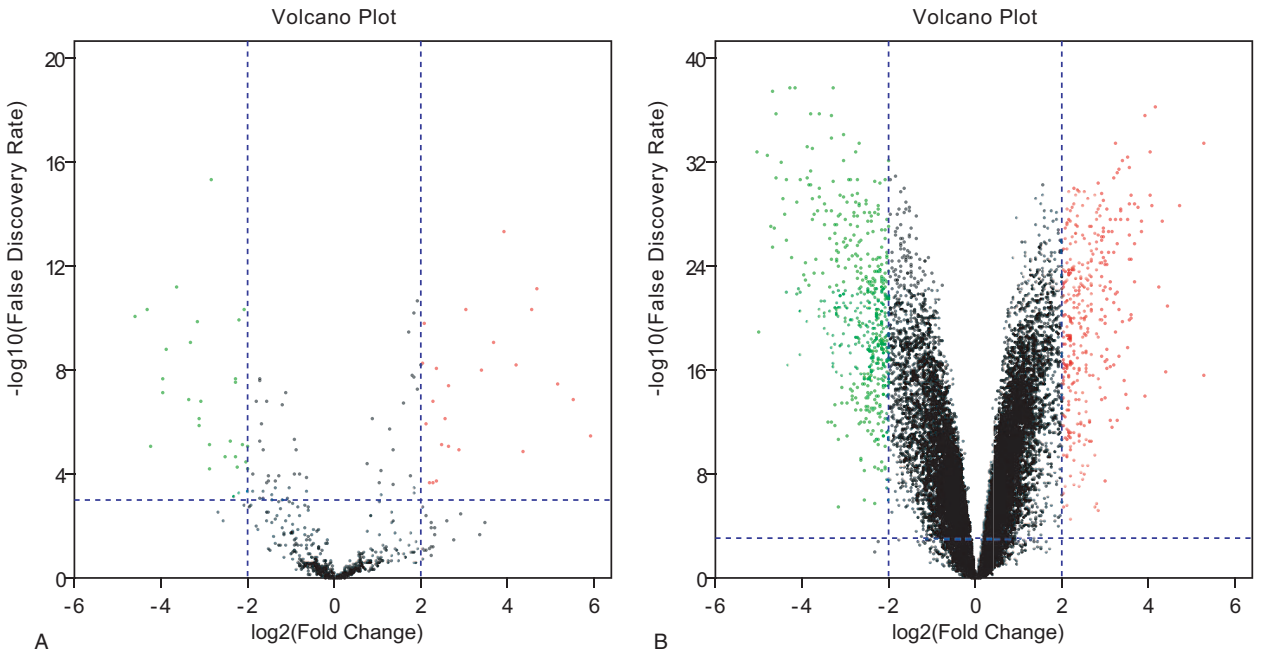

Figure 3. Volcano plot of the differentially expressed (DE) miRNAs (A) and DE-genes (B). (A) The black dots represent miRNAs that are not differentially expressed between 8 human normal lung samples and 35 human small cell lung cancer samples, and the red dots and green dots represent the upregulated and downregulated miRNAs in human small cell lung cancer samples, respectively. (B) The black dots represent genes that are not differentially expressed between 43 human normal lung samples and 15 human small cell lung cancer samples, and the red dots and green dots represent the upregulated and downregulated genes in human small cell lung cancer samples, respectively.

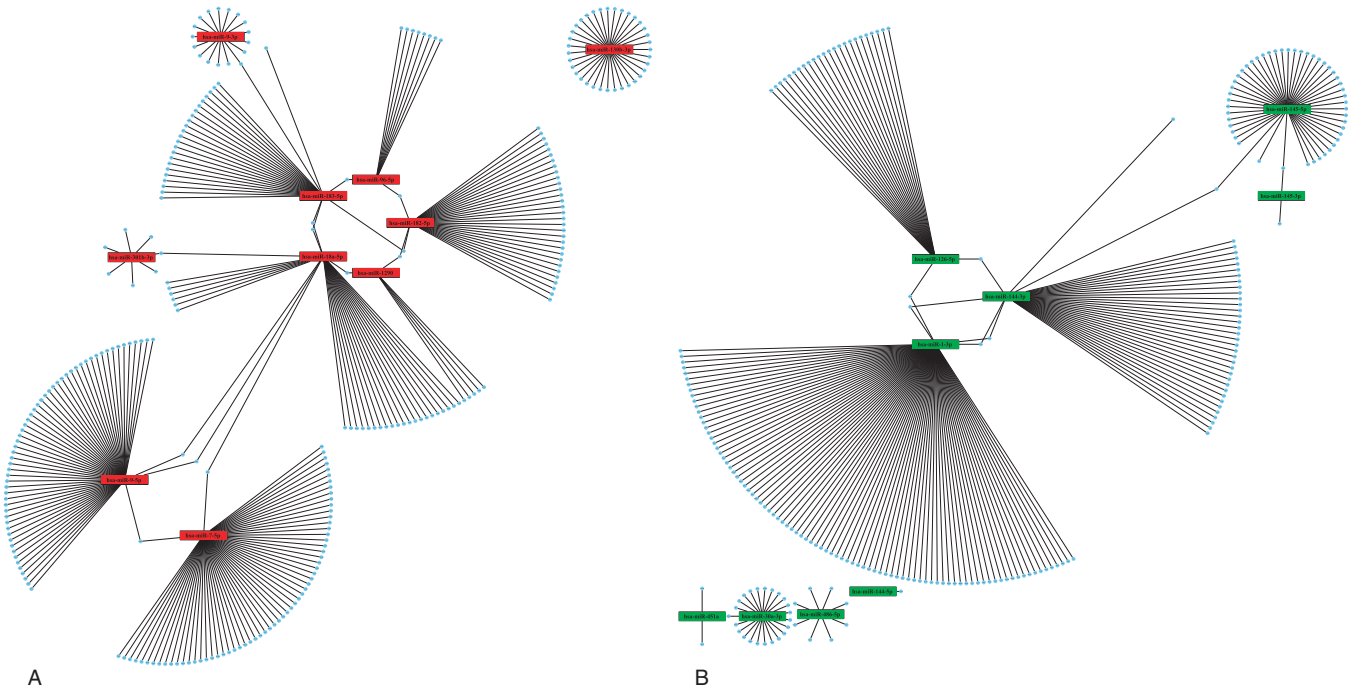

Figure 4. miRNAs-genes networks of top 10 upregulated and downregulated DE-miRNAs. (A) The network of the top 10 upregulated DE-miRNAs and their targets. (B) The network of the top 10 downregulated DE-miRNAs and their targets, because the 10th downregulated DE-miRNA hsa-miR-126-3p cannot find the same predicted target gene in the databases at the same time, so there is just nine genes in (B). DE = differentially expressed.

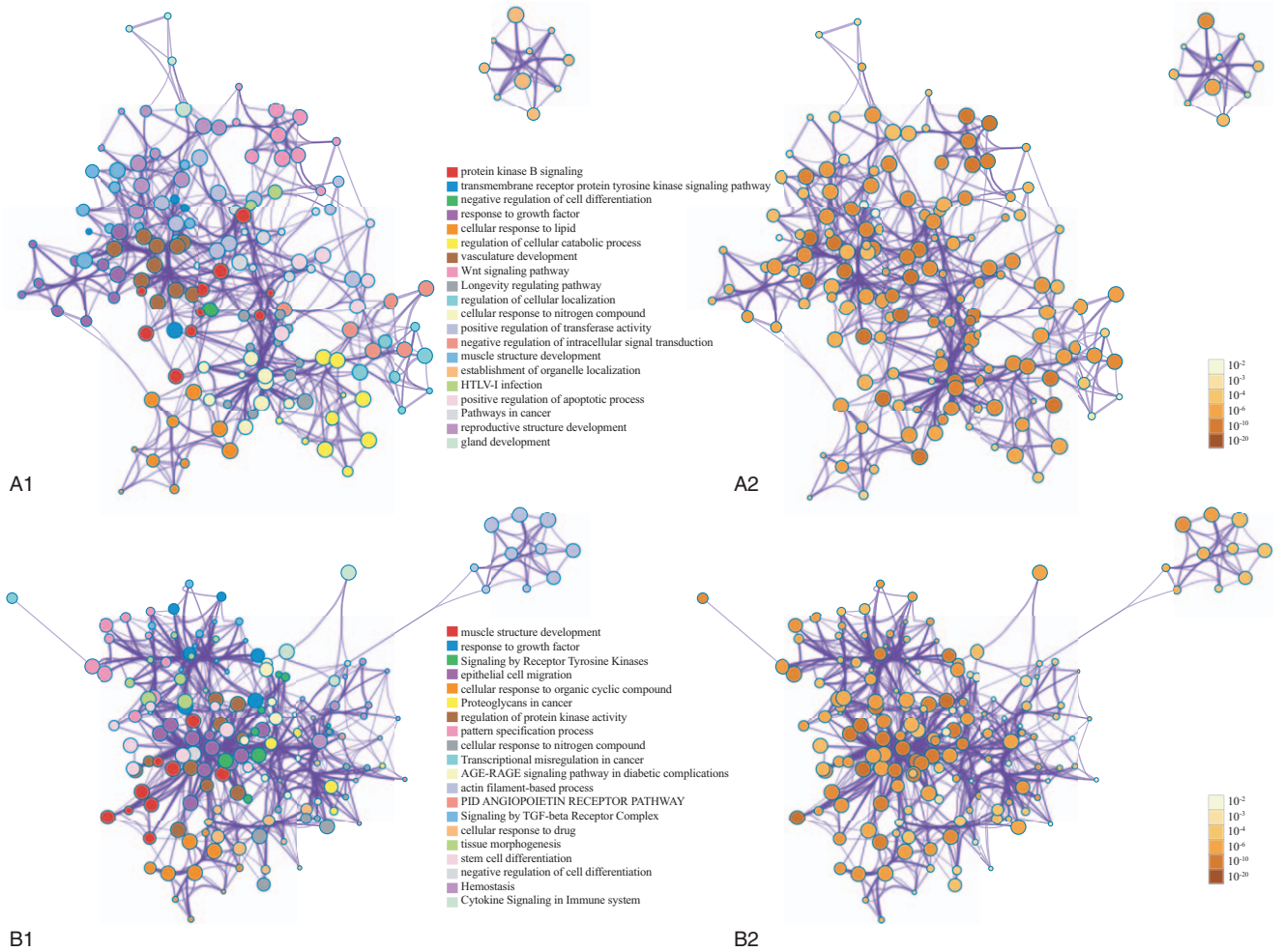

Figure 5. The visualized networks of enriched predicted target genes of top 10 upregulated and downregulated DE-miRNAs. (A) The visualized networks of enriched predicted target genes of top 10 upregulated DE-miRNAs, where each node represents an enriched term and is colored first by its cluster ID (A1) and then by its *P*-value (A2). (B) The visualized networks of enriched predicted target genes of top 10 downregulated DE-miRNAs, where each node represents an enriched term and is colored first by its cluster ID (B1) and then by its *P*-value (B2). DE = differentially expressed.

5. Discussion

Small-cell lung carcinoma has long been divided into two clinicopathological stages, including limited stage and extensive stage. The stage is generally determined by the presence or absence of metastases, whether or not the tumor appears limited to the thorax, and whether or not the entire tumor burden within the chest can feasibly be encompassed within a single radiotherapy portal. In general, if the tumor is confined to one lung and the lymph nodes close to that lung, the cancer is said to be limited stage. If the cancer has spread beyond that, it is said to be extensive stage.[14] In patients with extensive stage, median survival of 6 to 12 months is reported with currently available therapy, but long-term disease-free survival is rare.[2] Regardless of stage, the current prognosis for patients with SCLC is unsatisfactory despite improvements in diagnosis and therapy made during the past 25 years. Without treatment, SCLC has the most aggressive clinical course of any type of pulmonary tumor, with median survival from diagnosis of only 2 to 4 months. About 10% of the total population of SCLC patients remains free of disease during the 2 years from the start of therapy, which is the time period during which most relapses occur. Even these patients, however, are at risk of dying from lung cancer (both small and non-small cell types).[15] The overall survival at 5 years is 5% to 10%.[15–18]

In the medicine field, gene therapy is the therapeutic delivery of nucleic acid into a patient's cells as a drug to treat disease.[19] The first attempt at modifying human DNA was performed in 1980 by Martin Cline, but the first successful nuclear gene transfer in humans, approved by the National Institutes of Health, was performed in May 1989.[20] The possibility of correcting defective genes and modulating gene expression through gene therapy has emerged as a promising treatment strategy for cancer.[21] Furthermore, the relevance of tumor immune microenvironment in supporting the oncogenic process has paved the way for novel immunomodulatory applications of gene therapy.[21] Gene editing is a potential approach to alter the human genome to treat genetic diseases, viral diseases, and cancer.[22–24] The first commercial gene therapy, Gendicine, was approved in China in 2003 for the treatment of certain cancers.[25] Finding differential genes in cancerous and normal tissues is particularly important, but current genetic differences between SCLC and normal lung have rarely been reported.

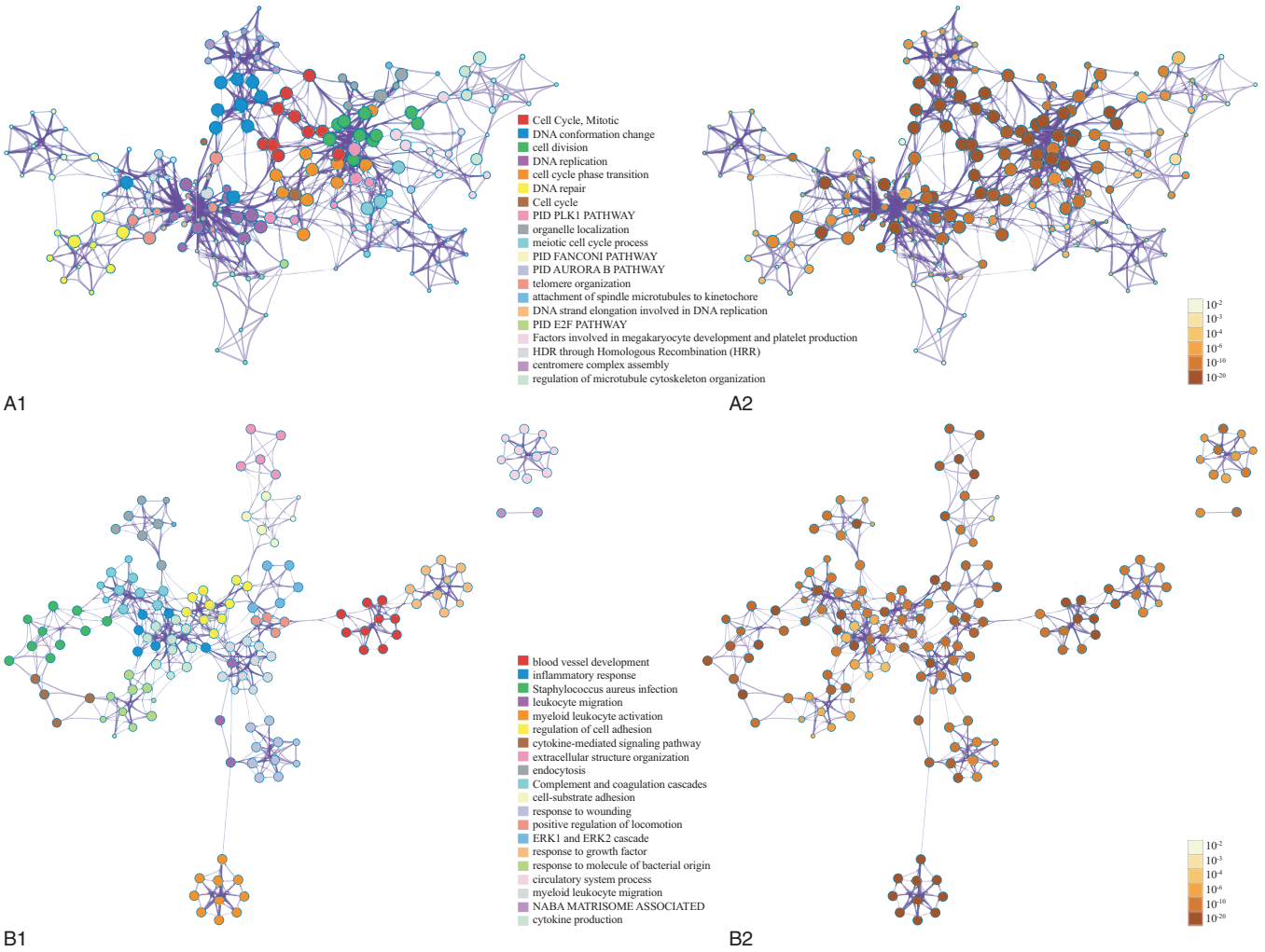

Figure 6. The visualized networks of enriched upregulated and downregulated DE-genes. (A) the visualized networks of upregulated DE-genes, where each node represents an enriched term and is colored first by its cluster ID (A1) and then by its *P*-value (A2). (B) The visualized networks of downregulated DE-genes, where each node represents an enriched term and is colored first by its cluster ID (B1) and then by its *P*-value (B2). DE = differentially expressed.

miRNAs are defined as small non-coding RNAs with a length of about 20 to 25 nucleotides, which exert pivotal effects in various biological processes.[26] miRNAs can regulate gene expression at post-transcriptional level through 3'-untranslated region (3' UTR) pairing with target gene mRNAs.[27] miRNAs regulate various targets which have critical roles in a wide spectrum of biological processes, including tumorigenesis and development, cell proliferation, metastasis, invasion, and apoptosis.[28] therefore, miRNA can be used as a potential and effective target for the diagnosis and treatment of a variety of tumors. In addition, the role of miRNA in the diagnosis and treatment of cancer provides a new strategy in the field of cancer therapy.[29,30] miR-30a-5p has been reported to inhibit the cell proliferation, invasion, migration, and autophagy in some types of tumors.[31,32] Xiang Yang et al found that Inhibition of Beclin-1 by induction of miR-30a-5p may improve the therapeutic outcome via resensitizing the drug-resistant cells to chemotherapy in SCLC.[33] Minting's team revealed that TSPAN12 promoted chemoresistance of SCLC under the regulation of miR-495.[34] More and more abnormal expressed miRNAs in different tumors have been reported, but fewer reports in SCLC till now. Deeper research is still to be done to find more miRNAs with differential expression SCLC and normal lung.

In our study, we screened an eligible gene dataset and an eligible miRNA dataset in the GEO database, and obtained the DE-genes or DE-miRNAs for each dataset by bioinformatics analysis, in this step, we choose the FDR criteria as <0.001 in order to gain more credible difference and less noise in the following steps. Then we performed target gene prediction on the top 10 DE-miRNAs, the intersection of predicted target genes and DE-genes was taken as the final DE-genes. Then apply the prediction miRNAs-targets relationship of top 10 DE-miRNAs to the final DE-genes to gain more convincing DE-miRNAs, DE-genes and their one to one relationship.

From the results of the Pathway and Process Enrichment Analysis, it can be seen that protein kinase B signaling, muscle structure development, Cell Cycle (Mitotic) and blood vessel development are more likely to be involved in the development of SCLC. Protein kinase B signaling has been found to be involved in the survival and proliferation of a variety of tumor cells,[35] including SCLC[36,37] and non–small-cell lung cancer (NSCLC) cells.[38] About muscle structure development, there are some of

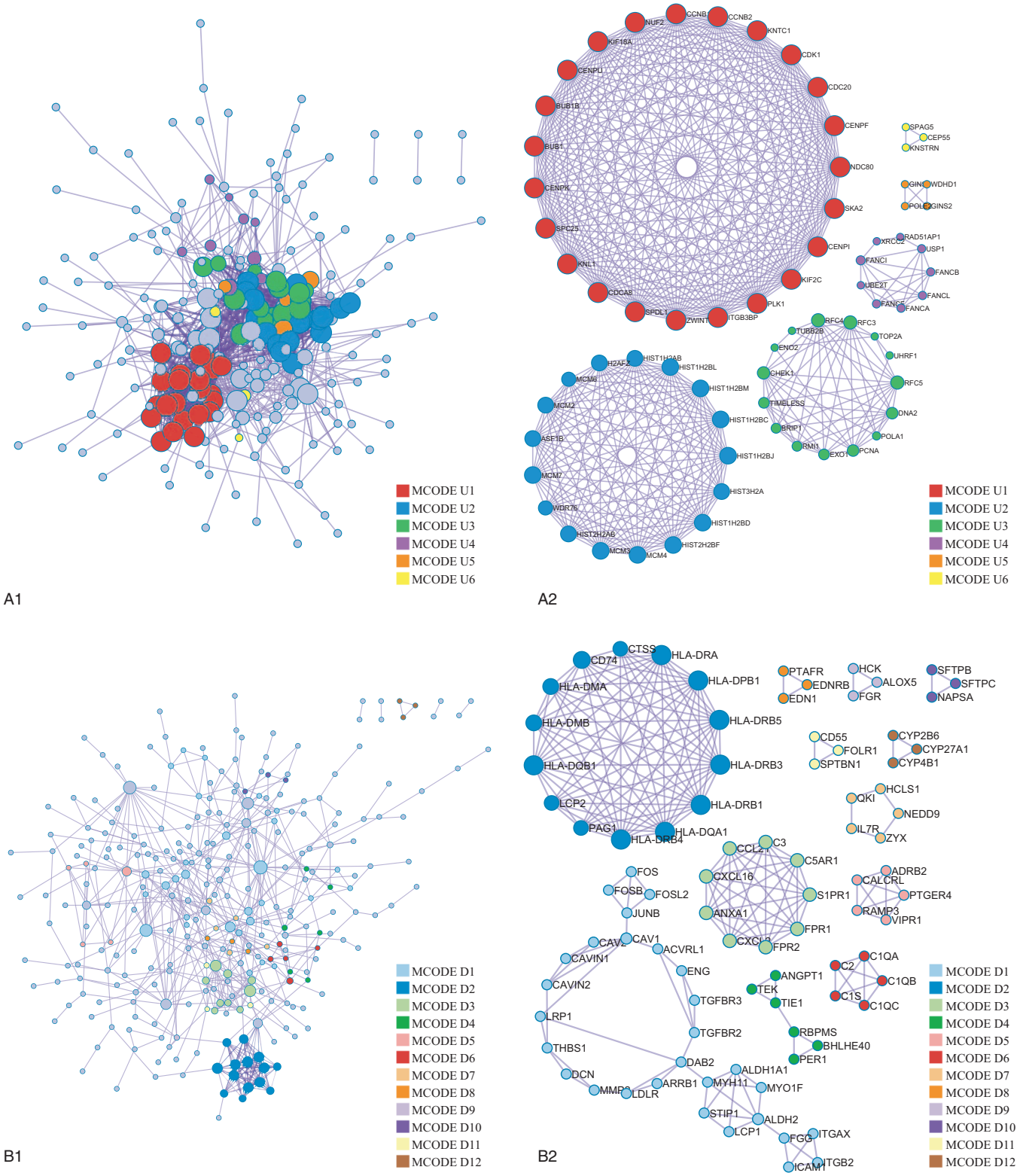

Figure 7. Visualized protein–protein interaction enrichment analysis of DE-genes. (A) Visualized protein–protein interaction enrichment of upregulated DE-genes. (B) Visualized protein–protein interaction enrichment of downregulated DE-genes. If the network contains between 3 and 500 proteins, the Molecular Complex Detection (MCODE) algorithm has been applied to identify densely connected network components. The MCODE networks identified for individual gene lists have been gathered and are shown in (A2) or (B2). DE = differentially expressed.

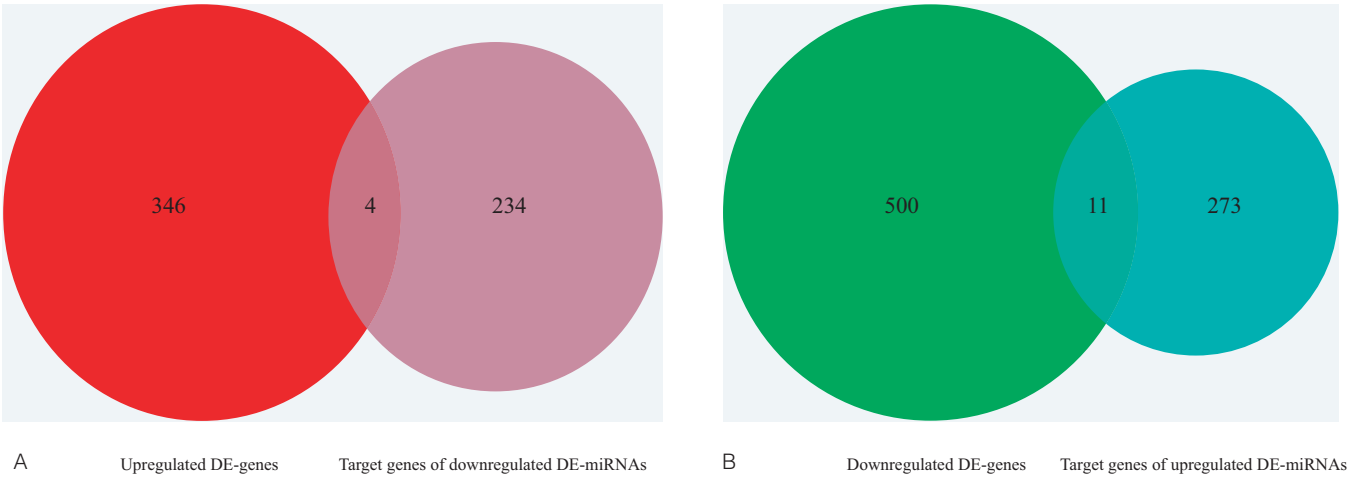

Figure 8. The intersections of DE-genes and the target genes of DE-miRNAs. (A) The intersection of upregulated DE-genes and the target genes of downregulated DE-miRNAs. (B) The intersection of downregulated DE-genes and the target genes of upregulated DE-miRNAs. DE = differentially expressed.

the more common paraneoplastic syndromes associated with lung cancer, such as syndrome of inappropriate anti-diuretic hormone (SIADH) and Nervous system problems, which will make muscle weakness or cramps.[39] The cell cycle, the process by which cells progress and divide, lies at the heart of cancer.[40] In cancer, as a result of genetic mutations, this regulatory process malfunctions, resulting in uncontrolled cell proliferation.[40] Yi's study demonstrated that asparagine synthetase had an important role in the growth of human lung cancer cells by inhibiting the proliferation and arresting the cell cycle of lung cancer cells.[41] Chengyu's team showed that Licochalcone A induces cell cycle arrest and apoptosis in lung cancer cells.[42] blood vessel development, also known as angiogenesis, it is an essential component in the microenvironment to tumor growth and metastasis, whereas inhibiting angiogenesis has become a promising strategy for cancer therapy.[43] VEGF overexpression and/or high VEGF serum levels have been reported both in non-small-cell lung carcinoma (NSCLC) and in SCLC.[44]

As we show them in Table 12, RBMS3, NEDD9, and CRIM1 are the top 3 downregulated genes in the small lung cancer tissue compared with normal lung. Their upstream miRNAs are hsa-miR-7–5p, hsa-miR-18a-5p, and hsa-miR-18a-5p, respectively. Recently, RBMS3 is found to be located at 3p24-p23, where is often found deleted or mutated in cancers, suggesting its potential role in tumor suppressing.[45] Yanan's team found that RBMS3 is a tumor suppressor gene that acts as a favorable prognostic marker in lung squamous cell carcinoma.[46] Chenglin reported that RBMS3 contributes to the tumorigenesis of lung

Table 2

The top 20 upregulated DE-miRNAs (ranked by |fold change [FC]|).

No.	row.names (tT)2	logFC	AveExpr	*t*	*P*	adj. *P* value	*B*	Regulated
1	hsa-miR-9–3p	5.915064	1.330272	6.094021	2.75E−07	3.24E−06	6.497889	Up-regulated
2	hsa-miR-1290	5.513574	2.114575	7.150232	8.17E−09	1.32E−07	9.967949	Up-regulated
3	hsa-miR-7-5p	5.150517	3.836668	7.65552	1.55E−09	2.99E−08	11.61341	Up-regulated
4	hsa-miR-183-5p	4.640001	3.027101	11.05447	4.23E−14	6.34E−12	21.9998	Up-regulated
5	hsa-miR-130b-3p	4.541749	3.302331	10.13871	6.25E−13	4.17E−11	19.34223	Up-regulated
6	hsa-miR-9-5p	4.352022	0.876776	5.635528	1.27E−06	1.17E−05	4.996322	Up-regulated
7	hsa-miR-301b-3p	4.195733	−0.00572	8.255081	2.21E−10	6.30E−09	13.54054	Up-regulated
8	hsa-miR-96-5p	3.916024	5.461447	13.12198	1.44E−16	4.32E−14	27.58495	Up-regulated
9	hsa-miR-182-5p	3.666389	0.222022	8.976073	2.22E−11	8.09E−10	15.81088	Up-regulated
10	hsa-miR-18a-5p	3.362656	2.038655	8.101559	3.62E−10	9.44E−09	13.05016	Up-regulated
11	hsa-miR-200b-3p	3.010067	7.009334	10.26818	4.24E−13	4.02E−11	19.72477	Up-regulated
12	hsa-miR-200a-5p	2.877382	0.297181	5.665468	1.15E−06	1.08E−05	5.09399	Up-regulated
13	hsa-miR-429	2.637601	5.148411	7.561255	2.11E−09	3.95E−08	11.30772	Up-regulated
14	hsa-miR-181c-3p	2.630176	0.029666	5.765868	8.22E−07	8.36E−06	5.421978	Up-regulated
15	hsa-miR-210	2.520739	3.751153	6.580643	5.43E−08	7.08E−07	8.098431	Up-regulated
16	hsa-miR-18b-5p	2.458106	0.801803	5.850226	6.21E−07	6.53E−06	5.698058	Up-regulated
17	hsa-miR-301a-3p	2.359574	4.5873	8.181012	2.80E−10	7.64E−09	13.30423	Up-regulated
18	hsa-miR-141-5p	2.336924	−0.71679	4.766887	2.20E−05	0.000163	2.206759	Up-regulated
19	hsa-miR-200a-3p	2.251327	5.955112	7.108071	9.39E−09	1.46E−07	9.82998	Up-regulated
20	hsa-miR-629-3p	2.247075	−0.27248	4.667387	3.03E−05	0.000209	1.894841	Up-regulated

DE = differentially expressed.

Table 3

The top 20 downregulated DE-miRNAs (ranked by |fold change [FC]|).

No.	row.names (tT)2	logFC	AveExpr	*t*	*P*	adj. *P* value	*B*	Regulated
1	hsa-miR-144-5p	−4.624300372	−1.046760099	−9.881056514	1.36E–12	7.41E–11	18.57445015	Down-regulated
2	hsa-miR-1-3p	−4.340794155	−1.477112646	−10.18097508	5.51E–13	4.13E–11	19.46735479	Down-regulated
3	hsa-miR-30a-3p	−4.260354557	−0.058575622	−5.754377022	8.54E–07	8.54E–06	5.384405266	Down-regulated
4	hsa-miR-144-3p	−3.994684449	3.072322266	−7.363648769	4.04E–09	6.92E–08	10.66489313	Down-regulated
5	hsa-miR-486-5p	−3.990005887	−0.57556997	−7.845250941	8.32E–10	1.92E–08	12.22661053	Down-regulated
6	hsa-miR-451a	−3.895519701	7.592862726	−8.76886158	4.27E–11	1.42E–09	15.16422935	Down-regulated
7	hsa-miR-126-5p	−3.655368436	−0.148090084	−11.17903707	2.96E–14	5.91E–12	22.35257096	Down-regulated
8	hsa-miR-145-5p	−3.393445083	2.223485789	−7.158216173	7.96E–09	1.32E–07	9.994067066	Down-regulated
9	hsa-miR-145-3p	−3.34441456	−1.555524692	−8.966549157	2.29E–11	8.09E–10	15.78126983	Down-regulated
10	hsa-miR-126-3p	−3.163321224	5.661856211	−9.663889496	2.63E–12	1.22E–10	17.92062666	Down-regulated
11	hsa-miR-338-3p	−3.151471897	2.901651144	−6.581439692	5.41E–08	7.08E–07	8.101051464	Down-regulated
12	hsa-miR-143-3p	−3.127310346	1.486364681	−6.398805586	9.95E–08	1.22E–06	7.500173957	Down-regulated
13	hsa-miR-572	−3.11513591	0.574523022	−7.104702089	9.50E–09	1.46E–07	9.818952064	Down-regulated
14	hsa-miR-139-5p	−2.919539687	−2.057906281	−5.133961696	6.65E–06	5.62E–05	3.373065874	Down-regulated
15	hsa-miR-30a-5p	−2.918076742	3.48383931	−5.867197048	5.86E–07	6.40E–06	5.753649644	Down-regulated
16	hsa-miR-30c-2-3p	−2.844327892	−2.84150328	−15.21910997	7.69E–19	4.61E–16	32.68634749	Down-regulated
17	hsa-miR-223-3p	−2.55367987	4.002522917	−5.469776476	2.20E–06	1.97E–05	4.456969259	Down-regulated
18	hsa-miR-133b	−2.404354083	−2.063368824	−5.943042447	4.55E–07	5.16E–06	6.002266651	Down-regulated
19	hsa-miR-150-5p	−2.35929296	2.210012514	−4.271275626	0.000106638	0.00063349	0.675470925	Down-regulated
20	hsa-miR-222-3p	−2.3459483	−0.702300768	−4.27474125	0.000105485	0.00063291	0.685965283	Down-regulated

DE = differentially expressed.

adenocarcinoma.[47] The upstream of RBMS3, hsa-miR-7-5p was reported to exert a tumor-suppressive function in glioblastoma and glioma by regulation of the EGFR, PI3K/ATK, Raf/MEK/ERK, and IGF-1R pathways.[48] NEDD9 has been identified as a pro-metastasis gene in several types of cancers including melanoma and breast cancer.[49] A recent article report that NEDD9 promotes lung cancer cell migration and invasion through the induction of epithelial-mesenchymal transition potentially via focal adhesion kinase activation.[49] Shunsuke's study showed that NEDD9 plays a pivotal role in cell metastasis and invasion of NSCLC cells, and expression of NEDD9 appears to be a promising biomarker for NSCLC prognosis.[50] The role of CRIM1 in controlling cancer cell behavior remains unknown.[51] Losing Hui's group treated the non-SCLC line A549 with CRIM1 peptide or RNA interference, they found that CRIM1 could promote the migration and adhesion of cancer cells significantly.[51] Turn to its upstream miRNA, hsa-miR-18a-5p can significantly reduce the hazard of dying for all cases, regardless of the tumor site.[52]

As in Table 13, KPNA2 (hsa-miR-144–3p), GPR137C (hsa-miR-1–3p), and GRIK3 (hsa-miR-144–3p) are the top 3 upregulated genes (upstream miRNAs) in the small lung cancer

Table 4

The top 20 upregulated DE-genes (ranked by |fold change [FC]|).

row.names (tT)	logFC	AveExpr	*t*	*P*	adj. *P* value	*B*	Regulated
BEX1	5.261001	4.845903	29.824	1.47E−37	2.78E−34	75.35792	Up-regulated
ASCL1	5.248224	5.065807	11.96659	1.68E−17	2.20E−16	29.27582	Up-regulated
TOP2A	4.703925	4.952057	23.53278	6.81E−32	2.02E−29	62.44423	Up-regulated
HIST1H3B	4.404367	7.362825	15.98388	3.08E−23	1.15E−21	42.52966	Up-regulated
HIST1H3C	4.39036	6.875054	12.12195	9.73E−18	1.32E−16	29.82673	Up-regulated
DCX	4.303129	4.665839	22.25454	1.37E−30	2.54E−28	59.45955	Up-regulated
HIST1H3I	4.208221	7.472089	17.28547	6.52E−25	3.41E−23	46.39314	Up-regulated
TUBB2B	4.134942	6.342362	34.10833	7.57E−41	4.00E−37	82.78514	Up-regulated
NUF2	4.052735	4.406568	23.56597	6.31E−32	1.89E−29	62.51992	Up-regulated
STMN1	4.021866	7.34713	28.93454	8.01E−37	1.17E−33	73.69038	Up-regulated
CENPF	4.012109	4.891905	24.49174	7.82E−33	3.23E−30	64.59531	Up-regulated
NOL4	3.911498	4.510551	10.846	9.66E−16	9.71E−15	25.21476	Up-regulated
CCNB1	3.885803	5.613738	32.62044	9.49E−40	2.51E−36	80.31239	Up-regulated
TPX2	3.838696	4.740715	21.39822	1.10E−29	1.68E−27	57.38048	Up-regulated
PRC1	3.834336	5.601847	22.26174	1.34E−30	2.51E−28	59.47676	Up-regulated
CCNB2	3.726617	4.856283	23.36728	9.97E−32	2.83E−29	62.06551	Up-regulated
FAM111B	3.677761	4.714654	17.68991	2.05E−25	1.21E−23	47.55346	Up-regulated
INA	3.646147	4.157539	20.39803	1.36E−28	1.64E−26	54.8663	Up-regulated
ASPM	3.644909	4.177032	23.76836	3.98E−32	1.33E−29	62.97947	Up-regulated
UCHL1	3.5919	6.765656	15.43391	1.67E−22	5.35E−21	40.83594	Up-regulated

DE = differentially expressed.

Table 5

The top 20 downregulated DE-genes (ranked by |fold change [FC]|).

row.names (tT)	logFC	AveExpr	*t*	*P*	Adj. *P* value	*B*	Regulated
AGER	−5.06587	9.599286	−28.8106	1.02E−36	1.41E−33	73.45434	Down-regulated
SFTPC	−5.01522	11.32473	−14.4585	3.66E−21	9.22E−20	37.7392	Down-regulated
ADH1B	−4.81084	7.817146	−28.4005	2.26E−36	2.84E−33	72.66636	Down-regulated
C4BPA	−4.75925	8.164412	−21.7203	4.98E−30	8.21E−28	58.17028	Down-regulated
CYP2B7P1	−4.68674	7.751528	−35.7826	4.94E−42	3.26E−38	85.44463	Down-regulated
AQP4	−4.68032	7.780042	−20.1321	2.71E−28	3.06E−26	54.18153	Down-regulated
LRRK2	−4.64208	7.718973	−21.6647	5.70E−30	9.24E−28	58.03465	Down-regulated
CLDN18	−4.63397	8.641473	−33.2212	3.38E−40	1.49E−36	81.32376	Down-regulated
FIGF	−4.61054	6.659177	−26.3134	1.54E−34	1.26E−31	68.4889	Down-regulated
GPRC5A	−4.48927	8.095534	−27.7322	8.49E−36	8.62E−33	71.35968	Down-regulated
NAPSA	−4.47272	8.795141	−24.2681	1.29E−32	5.00E−30	64.10021	Down-regulated
PGC	−4.40495	8.9249	−22.7554	4.15E−31	9.13E−29	60.64547	Down-regulated
SFTPB	−4.39776	11.03597	−16.9239	1.86E−24	8.84E−23	45.34	Down-regulated
FCN3	−4.39749	8.042272	−26.1382	2.23E−34	1.65E−31	68.12492	Down-regulated
SLC6A4	−4.37897	7.284032	−20.7092	6.17E−29	7.98E−27	55.65878	Down-regulated
LOC653879	−4.35257	9.327099	−12.5211	2.41E−18	3.61E−17	31.22814	Down-regulated
CLIC5	−4.31829	8.027221	−36.3338	2.06E−42	1.82E−38	86.29331	Down-regulated
STEAP4	−4.26722	6.983048	−19.4217	1.75E−27	1.70E−25	52.31808	Down-regulated
TCF21	−4.16799	8.053149	−37.1874	5.47E−43	1.44E−38	87.58261	Down-regulated
SLC34A2	−4.14461	10.11217	−16.7674	2.95E−24	1.33E−22	44.87935	Down-regulated

DE = differentially expressed.

tissue compared with normal lung. KPNA2 was identified as a potential biomarker for non-small-cell lung cancer (NSCLC) by integration of the cancer cell secretome and tissue transcriptome.[53] Xiaolei's study provided direct evidence to demonstrates that KPNA2 may contribute to nuclear translocation in lung cancer.[54] So far, we have not found any research and reports on the GPR137C gene, which may become an innovation and hot spot for future research. The expression of GRIK3 was found in rhabdomyosarcoma, neuroblastoma, thyroid tumor, lung cancer, breast cancer, astrocytoma, multiple myeloma, glioma, and colorectal cancer.[55] Meeta's team reported that GRIK3 gene was found to be methylated across all stages of lung adenocarcinoma, indicating that GRIK3 might be an epigenetic marker for diagnosis.[56] hsa-miR-144–3p was demonstrated that markedly elevated in serum of patients with hepatocellular carcinoma.[57] There is little literature on the relationship between hsa-miR-1–3p and cancer, and we believe this deserves more in-depth research.

Table 6

Top 20 clusters with their representative enriched terms of the targets genes of upregulated DE-miRNAs (one per cluster).

GO	Category	Description	Count	%	Log10(*P*)	Log10(*q*)
GO:0043491	GO biological processes	Protein kinase B signaling	21	7.394366197	−11.31600882	−7.381474527
GO:0007169	GO biological processes	Transmembrane receptor protein tyrosine kinase signaling pathway	35	12.32394366	−11.2673441	−7.381474527
GO:0045596	GO biological processes	Negative regulation of cell differentiation	35	12.32394366	−11.21572563	−7.381474527
GO:0070848	GO biological processes	Response to growth factor	35	12.32394366	−10.99533278	−7.286020409
GO:0071396	GO biological processes	Cellular response to lipid	31	10.91549296	−10.70062695	−7.088224591
GO:0031329	GO biological processes	Regulation of cellular catabolic process	35	12.32394366	−10.56995274	−7.074923026
GO:0001944	GO biological processes	Vasculature development	36	12.67605634	−10.54119735	−7.074923026
GO:0016055	GO biological processes	Wnt signaling pathway	27	9.507042254	−10.39303954	−7.03904561
hsa04211	KEGG pathway	Longevity regulating pathway	13	4.577464789	−10.02705107	−6.86180674
GO:0060341	GO biological processes	Regulation of cellular localization	35	12.32394366	−9.834504643	−6.699223541
GO:1901699	GO biological processes	Cellular response to nitrogen compound	31	10.91549296	−9.714369432	−6.607117053
GO:0051347	GO biological processes	Positive regulation of transferase activity	31	10.91549296	−9.453233039	−6.372309599
GO:1902532	GO biological processes	Negative regulation of intracellular signal transduction	27	9.507042254	−9.35571678	−6.345374413
GO:0061061	GO biological processes	Muscle structure development	30	10.56338028	−8.872635094	−5.955583669
GO:0051656	GO biological processes	Establishment of organelle localization	24	8.450704225	−8.443887011	−5.637664627
hsa05166	KEGG pathway	HTLV-I infection	18	6.338028169	−8.304231947	−5.511373525
GO:0043065	GO biological processes	Positive regulation of apoptotic process	28	9.85915493	−8.189721466	−5.446550828
hsa05200	KEGG pathway	Pathways in cancer	22	7.746478873	−8.138486493	−5.406897728
GO:0048608	GO biological processes	Reproductive structure development	22	7.746478873	−7.567524128	−4.954117607
GO:0048732	GO biological processes	Gland development	22	7.746478873	−7.424052382	−4.828683364

"Count" is the number of genes in the user-provided lists with membership in the given ontology term. "%" is the percentage of all of the user-provided genes that are found in the given ontology term (only input genes with at least one ontology term annotation are included in the calculation). "Log10(*P*)" is the *P*-value in log base 10. "Log10(*q*)" is the multi-test adjusted *P*-value in log base 10.
DE = differentially expressed.

Table 7

Top 20 clusters with their representative enriched terms of the targets genes of downregulated DE-miRNAs (one per cluster).

GO	Category	Description	Count	%	Log10(*P*)	Log10(*q*)
GO:0061061	GO biological processes	Muscle structure development	32	13.44537815	−12.21476634	−7.982366481
GO:0070848	GO biological processes	Response to growth factor	33	13.86554622	−11.81661759	−7.982366481
R-HSA-9006934	Reactome gene sets	Signaling by receptor tyrosine kinases	25	10.50420168	−10.70177324	−7.159946151
GO:0010631	GO biological processes	Epithelial cell migration	21	8.823529412	−10.05615035	−6.622401245
GO:0071407	GO biological processes	Cellular response to organic cyclic compound	26	10.92436975	−9.253602913	−6.197000324
hsa05205	KEGG pathway	Proteoglycans in cancer	16	6.722689076	−9.253100181	−6.197000324
GO:0045859	GO biological processes	Regulation of protein kinase activity	30	12.60504202	−8.959658578	−5.949316212
GO:0007389	GO biological processes	Pattern specification process	22	9.243697479	−8.685090472	−5.716140791
GO:1901699	GO biological processes	Cellular response to nitrogen compound	26	10.92436975	−8.254682169	−5.323521048
hsa05202	KEGG pathway	Transcriptional misregulation in cancer	14	5.882352941	−8.090158333	−5.205976183
hsa04933	KEGG pathway	AGE-RAGE signaling pathway in diabetic complications	11	4.62184874	−8.08598478	−5.205976183
GO:0030029	GO biological processes	Actin filament-based process	27	11.34453782	−7.817279964	−4.953065633
M92	Canonical Pathways	PID ANGIOPOIETIN RECEPTOR PATHWAY	8	3.361344538	−7.291770152	−4.548599515
R-HSA-170834	Reactome gene sets	Signaling by TGF-beta receptor complex	9	3.781512605	−7.113877031	−4.415288526
GO:0035690	GO biological processes	Cellular response to drug	17	7.142857143	−6.820460879	−4.233364387
GO:0048729	GO biological processes	Tissue morphogenesis	23	9.663865546	−6.693580631	−4.153060281
GO:0048863	GO biological processes	Stem cell differentiation	13	5.462184874	−6.611637406	−4.098249158
GO:0045596	GO biological processes	Negative regulation of cell differentiation	24	10.08403361	−6.232370437	−3.829483094
R-HSA-109582	Reactome gene sets	Hemostasis	22	9.243697479	−6.053374697	−3.688864304
R-HSA-1280215	Reactome gene sets	Cytokine signaling in immune system	23	9.663865546	−5.910224604	−3.590078318

"Count" is the number of genes in the user-provided lists with membership in the given ontology term. "%" is the percentage of all of the user-provided genes that are found in the given ontology term (only input genes with at least one ontology term annotation are included in the calculation). "Log10(*P*)" is the *P*-value in log base 10. "Log10(*q*)" is the multi-test adjusted *P*-value in log base 10.
DE = differentially expressed.

Most of the six differential genes and four differential miRNAs we have derived from the study have been confirmed by previous studies to be associated with lung cancer or cancer. But there are still some differential genes and miRs have not been explored, which may be the innovation of future research. Our study may provide potentially likely regulators of SCLC invasion and metastasis can serve as biomarkers in SCLC, also can give future researchers a broader perspective and more inspiration. But it still has limitations:

1. target gene prediction was performed only on the top 10 DE-miRNAs;

Table 8

Top 20 clusters with their representative enriched terms of the upregulated DE-genes (one per cluster).

GO	Category	Description	Count	%	Log10(*P*)	Log10(*q*)
R-HSA-69278	Reactome gene sets	Cell cycle, mitotic	85	25.07374631	−62.56476004	−58.25338768
GO:0071103	GO biological processes	DNA conformation change	46	13.56932153	−34.56578594	−30.95338358
GO:0051301	GO biological processes	Cell division	60	17.69911504	−32.50620884	−28.97298773
GO:0006260	GO biological processes	DNA replication	39	11.50442478	−26.98023889	−23.92413904
GO:0044770	GO biological processes	Cell cycle phase transition	50	14.74926254	−24.31130804	−21.32215498
GO:0006281	GO biological processes	DNA repair	46	13.56932153	−20.97913394	−18.18627551
hsa04110	KEGG pathway	Cell cycle	22	6.489675516	−17.13334146	−14.58539709
M129	Canonical pathways	PID PLK1 pathway	15	4.424778761	−16.14594534	−13.7210637
GO:0051640	GO biological processes	Organelle localization	39	11.50442478	−13.22502945	−10.97811508
GO:1903046	GO biological processes	Meiotic cell cycle process	22	6.489675516	−13.16991865	−10.92673215
M1	Canonical pathways	PID fanconi pathway	13	3.83480826	−13.01593186	−10.78010646
M14	Canonical pathways	PID aurora B pathway	12	3.539823009	−12.679937	−10.45846975
GO:0032200	GO biological processes	Telomere organization	20	5.899705015	−12.10954371	−9.89854189
GO:0008608	GO biological processes	Attachment of spindle microtubules to kinetochore	10	2.949852507	−10.58244466	−8.41095138
GO:0006271	GO biological processes	DNA strand elongation involved in DNA replication	8	2.359882006	−10.38938766	−8.230303643
M40	Canonical pathways	PID E2F PATHWAY	13	3.83480826	−10.2979287	−8.150909197
R-HSA-983231	Reactome gene sets	Factors involved in megakaryocyte development and platelet production	18	5.309734513	−10.26787369	−8.123818665
R-HSA-5685942	Reactome gene sets	HDR through Homologous Recombination (HRR)	12	3.539823009	−9.652991053	−7.540275778
GO:0034508	GO biological processes	Centromere complex assembly	11	3.244837758	−9.349920498	−7.26071991
GO:0070507	GO biological processes	Regulation of microtubule cytoskeleton organization	17	5.014749263	−9.100980948	−7.014917868

"Count" is the number of genes in the user-provided lists with membership in the given ontology term. "%" is the percentage of all of the user-provided genes that are found in the given ontology term (only input genes with at least one ontology term annotation are included in the calculation). "Log10(*P*)" is the *P*-value in log base 10. "Log10(*q*)" is the multi-test adjusted *P*-value in log base 10.
DE = differentially expressed.

Table 9

Top 20 clusters with their representative enriched terms of the downregulated DE-genes (one per cluster).

GO	Category	Description	Count	%	Log10(*P*)	Log10(*q*)
GO:0001568	GO biological processes	Blood vessel development	81	16.46341463	−33.38812498	−29.07675262
GO:0006954	GO biological processes	Inflammatory response	79	16.05691057	−31.61788189	−27.95877493
hsa05150	KEGG pathway	*Staphylococcus aureus* infection	28	5.691056911	−31.57117728	−27.95877493
GO:0050900	GO biological processes	Leukocyte migration	56	11.38211382	−25.13495122	−21.72666884
GO:0002274	GO biological processes	Myeloid leukocyte activation	64	13.00813008	−25.0467172	−21.68958735
GO:0030155	GO biological processes	Regulation of cell adhesion	64	13.00813008	−24.29051149	−20.97913913
GO:0019221	GO biological processes	Cytokine-mediated signaling pathway	67	13.61788618	−23.58604751	−20.35385639
GO:0043062	GO biological processes	Extracellular structure organization	50	10.16260163	−23.47154154	−20.30629721
GO:0006897	GO biological processes	Endocytosis	63	12.80487805	−19.78923779	−16.9111801
hsa04610	KEGG pathway	Complement and coagulation cascades	23	4.674796748	−19.52264915	−16.68839804
GO:0031589	GO biological processes	Cell-substrate adhesion	40	8.130081301	−18.43456264	−15.64170422
GO:0009611	GO biological processes	Response to wounding	56	11.38211382	−18.18920228	−15.40930883
GO:0040017	GO biological processes	Positive regulation of locomotion	50	10.16260163	−17.71214516	−14.94484084
GO:0070371	GO biological processes	ERK1 and ERK2 cascade	39	7.926829268	−17.09502995	−14.36344119
GO:0070848	GO biological processes	Response to growth factor	57	11.58536585	−16.97593537	−14.266623
GO:0002237	GO biological processes	Response to molecule of bacterial origin	37	7.520325203	−16.00188304	−13.41478655
GO:0003013	GO biological processes	Circulatory system process	44	8.943089431	−14.58708333	−12.04656298
GO:0097529	GO biological processes	Myeloid leukocyte migration	27	5.487804878	−14.08224736	−11.55620483
M5885	Canonical pathways	NABA matrisome associated	53	10.77235772	−13.72744284	−11.22225045
GO:0001816	GO biological processes	Cytokine production	50	10.16260163	−13.23170035	−10.75917708

"Count" is the number of genes in the user-provided lists with membership in the given ontology term. "%" is the percentage of all of the user-provided genes that are found in the given ontology term (only input genes with at least one ontology term annotation are included in the calculation). "Log10(*P*)" is the *P*-value in log base 10. "Log10(*q*)" is the multi-test adjusted *P*-value in log base 10.
DE = differentially expressed.

2. Only target genes of the top 10 DE-miRNAs are selected for further enrichment analysis;
3. A lack of experimental verification, more studies should be performed.

6. Conclusion

In conclusion, we have successfully identified differential expression of genes (RBMS3, NEDD9, CRIM1, TGFBR2, MYO1C, KLF4, EMP2, TMEM2, CTGF, TNFAIP3, THBS1, KPNA2, GPR137C, GRIK3, and MTHFD2) and upstream miRNAs (hsa-miR-7–5p, hsa-miR-18a-5p, hsa-miR-18a-5p, hsa-miR-9–5p, hsa-miR-9–5p, hsa-miR-7–5p, hsa-miR-1290, hsa-miR-18a-5p, hsa-miR-18a-5p, hsa-miR-18a-5p, hsa-miR-182–5p, hsa-miR-144–3p, hsa-miR-1–3p, hsa-miR-144–3p, and hsa-miR-30a-3p) in SCLC based on bioinformatic analysis. At the same time, we found that the DE-genes (RBMS3, NEDD9, CRIM1, KPNA2, GPR137C, and GRIK3), hsa-miR-7–5p, hsa-miR-18a-5p, hsa-miR-144–3p, hsa-miR-1–3p, and the protein kinase B signaling, muscle structure development, Cell Cycle

Table 10

Protein–protein interaction enrichment analysis.

MCODE	GO	Description	Log10(*P*)
MCODE U1	R-HSA-2500257	Resolution of sister chromatid cohesion	−53
MCODE U1	R-HSA-68877	Mitotic prometaphase	−48.1
MCODE U1	R-HSA-141424	Amplification of signal from the kinetochores	−45.4
MCODE U2	hsa05322	Systemic lupus erythematosus	−18.3
MCODE U2	R-HSA-3214815	HDACs deacetylate histones	−17.3
MCODE U2	GO:0071103	DNA conformation change	−17.3
MCODE U3	R-HSA-5685942	HDR through Homologous Recombination (HRR)	−19.4
MCODE U3	R-HSA-5693567	HDR through Homologous Recombination (HRR) or Single Strand Annealing (SSA)	−19.1
MCODE U3	R-HSA-5693538	Homology directed repair	−18.9
MCODE U4	R-HSA-6783310	Fanconi anemia pathway	−18
MCODE U4	M1	PID Fanconi pathway	−17.5
MCODE U4	GO:0036297	interstrand cross-link repair	−17.3
MCODE U5	GO:0006261	DNA-dependent DNA replication	−8.8
MCODE U5	GO:0006260	DNA replication	−7.8
MCODE U5	R-HSA-69239	Synthesis of DNA	−6.3
MCODE U6	GO:0000070	Mitotic sister chromatid segregation	−6.6
MCODE U6	GO:0000819	Sister chromatid segregation	−6.3
MCODE U6	GO:0098813	Nuclear chromosome segregation	−5.9

Protein–protein interaction enrichment analysis has been applied to each Molecular Complex Detection (MCODE) component of upregulated DE-genes independently, and the three best-scoring terms by *P*-value have been retained as the functional description of the corresponding components, all MCODEs are ranked by their |Log10(*P*)|.
DE = differentially expressed.

Table 11

Protein-protein interaction enrichment analysis.

MCODE	GO	Description	Log10(*P*)
MCODE D1	GO:0030198	Extracellular matrix organization	−12.7
MCODE D1	GO:0043062	Extracellular structure organization	−12
MCODE D1	GO:0007179	Transforming growth factor beta receptor signaling pathway	−11.9
MCODE D2	hsa04612	Antigen processing and presentation	−28.2
MCODE D2	GO:0019886	Antigen processing and presentation of exogenous peptide antigen via MHC class II	−26.8
MCODE D2	GO:0002495	Antigen processing and presentation of peptide antigen via MHC class II	−26.7
MCODE D3	R-HSA-373076	Class A/1 (Rhodopsin-like receptors)	−16.8
MCODE D3	R-HSA-418594	G alpha (i) signalling events	−16
MCODE D3	R-HSA-375276	Peptide ligand-binding receptors	−15.8
MCODE D4	GO:0043408	Regulation of MAPK cascade	−4.8
MCODE D4	GO:0070374	Positive regulation of ERK1 and ERK2 cascade	−4.7
MCODE D4	GO:0070372	Regulation of ERK1 and ERK2 cascade	−4.3
MCODE D5	GO:0007187	G-protein coupled receptor signaling pathway, coupled to cyclic nucleotide second messenger	−9.9
MCODE D5	GO:0007189	Adenylate cyclase-activating G-protein coupled receptor signaling pathway	−8.6
MCODE D5	R-HSA-500792	GPCR ligand binding	−8.5
MCODE D6	R-HSA-166663	Initial triggering of complement	−15.2
MCODE D6	R-HSA-173623	Classical antibody-mediated complement activation	−14.2
MCODE D6	R-HSA-977606	Regulation of complement cascade	−13.6
MCODE D7	GO:0007015	Actin filament organization	−4.3
MCODE D7	GO:0030036	Actin cytoskeleton organization	−3.7
MCODE D7	GO:0097435	Supramolecular fiber organization	−3.7
MCODE D8	GO:0051930	Regulation of sensory perception of pain	−8.4
MCODE D8	GO:0051931	Regulation of sensory perception	−8.3
MCODE D8	GO:0042310	Vasoconstriction	−7.3
MCODE D9	GO:0043299	Leukocyte degranulation	−4.9
MCODE D9	GO:0045055	Regulated exocytosis	−4.5
MCODE D10	R-HSA-5683826	Surfactant metabolism	−8.7
MCODE D11	R-HSA-6807878	COPI-mediated anterograde transport	−7.1
MCODE D11	R-HSA-199977	ER to Golgi anterograde Transport	−6.5
MCODE D11	R-HSA-948021	Transport to the Golgi and subsequent modification	−6.3
MCODE D12	R-HSA-211897	Cytochrome P450 - arranged by substrate type	−7.7
MCODE D12	R-HSA-211945	Phase I–Functionalization of compounds	−7
MCODE D12	R-HSA-211859	Biological oxidations	−6.1

Protein-protein interaction enrichment analysis has been applied to each Molecular Complex Detection (MCODE) component of downregulated DE-genes independently, and the three best-scoring terms by p-value have been retained as the functional description of the corresponding components, all MCODEs are ranked by their |Log10(*P*)|.
DE = differentially expressed.

Table 12

More convinced downregulated DE- genes and their upstream miRNAs.

Gene symbol	miRNA
RBMS3	hsa-miR-7-5p
NEDD9	hsa-miR-18a-5p
CRIM1	hsa-miR-18a-5p
TGFBR2	hsa-miR-9-5p
MYO1C	hsa-miR-9-5p
KLF4	hsa-miR-7-5p
EMP2	hsa-miR-1290
TMEM2	hsa-miR-18a-5p
CTGF	hsa-miR-18a-5p
TNFAIP3	hsa-miR-18a-5p
THBS1	hsa-miR-182-5p

DE = differentially expressed.

(Mitotic) and blood vessel development are highly likely to be related to the SCLC. Undoubtedly, continued efforts to delineate the mechanism of differential genes and miRNAs will reveal novel insights into SCLC.

Table 13

More convinced upregulated DE- genes and their upstream miRNAs.

Gene symbol	miRNA
KPNA2	hsa-miR-144-3p
GPR137C	hsa-miR-1-3p
GRIK3	hsa-miR-144-3p
MTHFD2	hsa-miR-30a-3p

DE = differentially expressed.

Acknowledgments

Thanks to the reviewers for their valuable comments and suggestions that helped improve the quality of our manuscript.

Author contributions

Resources: Jian Zhang.
Visualization: Huan Luo.
Writing – original draft: Xiuwei Li, Chao Ma.
Writing – review & editing: Jinan Wang, Hongtao Guo.

References

[1] Joshi M, Ayoola A, Belani CP. Small-cell lung cancer: an update on targeted therapies. Adv Exp Med Biol 2013;779:385–404.
[2] Small Cell Lung Cancer Treatment (PDQ(R)): Health Professional Version. *PDQ Cancer Information Summaries*. Bethesda, MD; 2002.
[3] Jemal A, Center MM, DeSantis C, et al. Global patterns of cancer incidence and mortality rates and trends. Cancer Epidemiol Biomarkers Prev 2010;19:1893–907.
[4] Sorensen M, Pijls-Johannesma M, Felip E, et al. Small-cell lung cancer: ESMO Clinical Practice Guidelines for diagnosis, treatment and follow-up. Ann Oncol 2010;21(Suppl 5):v120–5.
[5] Arcaro A. Targeted therapies for small cell lung cancer: where do we stand? Crit Rev Oncol Hematol 2015;95:154–64.
[6] Bartel DP. MicroRNAs: target recognition and regulatory functions. Cell 2009;136:215–33.
[7] Shukla GC, Singh J, Barik S. MicroRNAs: processing, maturation, target recognition and regulatory functions. Mol Cell Pharmacol 2011;3:83–92.
[8] Uddin A, Chakraborty S. Role of miRNAs in lung cancer. J Cell Physiol 2018;doi: 10.1002/jcp.26607.
[9] Du L. Pertsemlidis A. microRNA regulation of cell viability and drug sensitivity in lung cancer. Expert Opin Biol Ther 2012;12:1221–39.
[10] Barrett T, Wilhite SE, Ledoux P, et al. NCBI GEO: archive for functional genomics data sets—update. Nucleic Acids Res 2013;41(Database issue): D991–995.
[11] Zar JH. Biostatistical Analysis. New Delhi, India: Pearson Education India; 1999.
[12] Hochberg Y, Benjamini Y. More powerful procedures for multiple significance testing. Stat Med 1990;9:811–8.
[13] McHugh ML. Interrater reliability: the kappa statistic. Biochem Med (Zagreb) 2012;22:276–82.
[14] Argiris A, Murren JR. Staging and clinical prognostic factors for small-cell lung cancer. Cancer J 2001;7:437–47.
[15] Johnson BE, Grayson J, Makuch RW, et al. Ten-year survival of patients with small-cell lung cancer treated with combination chemotherapy with or without irradiation. J Clin Oncol 1990;8:396–401.
[16] Fry WA, Menck HR, Winchester DP. The National Cancer Data Base report on lung cancer. Cancer 1996;77:1947–55.
[17] Lassen U, Osterlind K, Hansen M, et al. Long-term survival in small-cell lung cancer: posttreatment characteristics in patients surviving 5 to 18+ years—an analysis of 1,714 consecutive patients. J Clin Oncol 1995;13:1215–20.
[18] Murray N, Coy P, Pater JL, et al. Importance of timing for thoracic irradiation in the combined modality treatment of limited-stage small-cell lung cancer. The National Cancer Institute of Canada Clinical Trials Group. J Clin Oncol 1993;11:336–44.
[19] Kaji EH, Leiden JM. Gene and stem cell therapies. JAMA 2001;285:545–50.
[20] Rosenberg SA, Aebersold P, Cornetta K, et al. Gene transfer into humans—immunotherapy of patients with advanced melanoma, using tumor-infiltrating lymphocytes modified by retroviral gene transduction. N Engl J Med 1990;323:570–8.
[21] Bottai G, Truffi M, Corsi F, et al. Progress in nonviral gene therapy for breast cancer and what comes next? Expert Opin Biol Ther 2017;17:595–611.
[22] Porteus M. Genome editing: a new approach to human therapeutics. Annu Rev Pharmacol Toxicol 2016;56:163–90.
[23] Stone D, Niyonzima N, Jerome KR. Genome editing and the next generation of antiviral therapy. Hum Genet 2016;135:1071–82.
[24] Khan FA, Pandupuspitasari NS, Chun-Jie H, et al. CRISPR/Cas9 therapeutics: a cure for cancer and other genetic diseases. Oncotarget 2016;7:52541–52.
[25] Pearson S, Jia H, Kandachi K. China approves first gene therapy. Nat Biotechnol 2004;22:3–4.
[26] Mallory AC, Vaucheret H. MicroRNAs: something important between the genes. Curr Opin Plant Biol 2004;7:120–5.
[27] Bartel DP. MicroRNAs: genomics, biogenesis, mechanism, and function. Cell 2004;116:281–97.
[28] Hwang HW, Mendell JT. MicroRNAs in cell proliferation, cell death, and tumorigenesis. Br J Cancer 2006;94:776–80.
[29] Long W, Zhao C, Ji C, et al. Characterization of serum microRNAs profile of PCOS and identification of novel non-invasive biomarkers. Cell Physiol Biochem 2014;33:1304–15.
[30] Wang QX, Zhu YQ, Zhang H, et al. Altered MiRNA expression in gastric cancer: a systematic review and meta-analysis. Cell Physiol Biochem 2015;35:933–44.
[31] Zhao JJ, Lin J, Zhu D, et al. miR-30-5p functions as a tumor suppressor and novel therapeutic tool by targeting the oncogenic Wnt/beta-catenin/BCL9 pathway. Cancer Res 2014;74:1801–13.
[32] Yang X, Chen Y, Chen L. The versatile role of microRNA-30a in human cancer. Cell Physiol Biochem 2017;41:1616–32.
[33] Yang X, Bai F, Xu Y, et al. Intensified Beclin-1 mediated by low expression of Mir-30a-5p promotes chemoresistance in human small cell lung cancer. Cell Physiol Biochem 2017;43:1126–39.
[34] Ye M, Wei T, Wang Q, et al. TSPAN12 promotes chemoresistance and proliferation of SCLC under the regulation of miR-495. Biochem Biophys Res Commun 2017;486:349–56.
[35] Chang F, Lee JT, Navolanic PM, et al. Involvement of PI3K/Akt pathway in cell cycle progression, apoptosis, and neoplastic transformation: a target for cancer chemotherapy. Leukemia 2003;17:590–603.
[36] Kraus AC, Ferber I, Bachmann SO, et al. In vitro chemo- and radio-resistance in small cell lung cancer correlates with cell adhesion and constitutive activation of AKT and MAP kinase pathways. Oncogene 2002;21:8683–95.
[37] Krystal GW, Sulanke G, Litz J. Inhibition of phosphatidylinositol 3-kinase-Akt signaling blocks growth, promotes apoptosis, and enhances sensitivity of small cell lung cancer cells to chemotherapy. Mol Cancer Ther 2002;1:913–22.
[38] Brognard J, Clark AS, Ni Y, et al. Akt/protein kinase B is constitutively active in non-small cell lung cancer cells and promotes cellular survival and resistance to chemotherapy and radiation. Cancer Res 2001;61:3986–97.
[39] Gandhi L, Johnson BE. Paraneoplastic syndromes associated with small cell lung cancer. J Natl Compr Canc Netw 2006;4:631–8.
[40] Vermeulen K, Van Bockstaele DR, Berneman ZN. The cell cycle: a review of regulation, deregulation and therapeutic targets in cancer. Cell Prolif 2003;36:131–49.
[41] Xu Y, Lv F, Zhu X, et al. Loss of asparagine synthetase suppresses the growth of human lung cancer cells by arresting cell cycle at G0/G1 phase. Cancer Gene Ther 2016;23:287–94.
[42] Qiu C, Zhang T, Zhang W, et al. Licochalcone A inhibits the proliferation of human lung cancer cell lines A549 and H460 by inducing G2/M cell cycle arrest and ER stress. Int J Mol Sci 2017;18:
[43] Weis SM, Cheresh DA. Tumor angiogenesis: molecular pathways and therapeutic targets. Nat Med 2011;17:1359–70.
[44] Alevizakos M, Kaltsas S, Syrigos KN. The VEGF pathway in lung cancer. Cancer Chemother Pharmacol 2013;72:1169–81.
[45] Penkov D, Ni R, Else C, et al. Cloning of a human gene closely related to the genes coding for the c-myc single-strand binding proteins. Gene 2000;243:27–36.
[46] Liang YN, Liu Y, Meng Q, et al. RBMS3 is a tumor suppressor gene that acts as a favorable prognostic marker in lung squamous cell carcinoma. Med Oncol 2015;32:459.
[47] Liu C, Zhang YH, Huang T, et al. Identification of transcription factors that may reprogram lung adenocarcinoma. Artif Intell Med 2017;83:52–7.
[48] Li G, Huang M, Cai Y, et al. Circ-U2AF1 promotes human glioma via derepressing neuro-oncological ventral antigen 2 by sponging hsa-miR-7-5p. J Cell Physiol 2019;234:9144–55.
[49] Jin Y, Li F, Zheng C, et al. NEDD9 promotes lung cancer metastasis through epithelial-mesenchymal transition. Int J Cancer 2014;134:2294–304.
[50] Kondo S, Iwata S, Yamada T, et al. Impact of the integrin signaling adaptor protein NEDD9 on prognosis and metastatic behavior of human lung cancer. Clin Cancer Res 2012;18:6326–38.
[51] Zeng H, Zhang Y, Yi Q, et al. CRIM1, a newfound cancer-related player, regulates the adhesion and migration of lung cancer cells. Growth Factors 2015;33:384–92.
[52] Slattery ML, Herrick JS, Mullany LE, et al. An evaluation and replication of miRNAs with disease stage and colorectal cancer-specific mortality. Int J Cancer 2015;137:428–38.
[53] Wang CI, Wang CL, Wang CW, et al. Importin subunit alpha-2 is identified as a potential biomarker for non-small cell lung cancer by integration of the cancer cell secretome and tissue transcriptome. Int J Cancer 2011;128:2364–72.
[54] Li XL, Jia LL, Shi MM, et al. Downregulation of KPNA2 in non-small-cell lung cancer is associated with Oct4 expression. J Transl Med 2013;11:232.
[55] Stepulak A, Luksch H, Gebhardt C, et al. Expression of glutamate receptor subunits in human cancers. Histochem Cell Biol 2009;132:435–45.
[56] Pradhan MP, Desai A, Palakal MJ. Systems biology approach to stage-wise characterization of epigenetic genes in lung adenocarcinoma. BMC Syst Biol 2013;7:141.
[57] Pu C, Huang H, Wang Z, et al. Extracellular vesicle-associated mir-21 and mir-144 are markedly elevated in serum of patients with hepatocellular carcinoma. Front Physiol 2018;9:930.